Antimicrobial resistance as a signature of soil restoration across a 143-year chronosequence

Short title: AMR as a soil health signature

Authors and affiliations:

Tim Goodall[1,*], Briony Jones[2], Amy C. Thorpe[1], Robert I. Griffiths[3], Hyun S. Gweon[4], Daniel S. Read[1], Richard Pywell[1], Susheel Bhanu Busi[1,*]

[1]UK Centre for Ecology & Hydrology, Benson Lane, Wallingford, UK

[2]UK Centre for Ecology & Hydrology, Deiniol Road, Bangor, UK

[3]School of Environment, Bangor University, Bangor, UK

[4]School of Biological Sciences, University of Reading, Reading, UK

*Corresponding authors:

Tim Goodall, timgoo@ceh.ac.uk, UK Centre for Ecology & Hydrology, Benson Lane, Crowmarsh Gifford, Wallingford, OX10 8BB, UK

Susheel Bhanu Busi, susbus@ceh.ac.uk, UK Centre for Ecology & Hydrology, Benson Lane, Crowmarsh Gifford, Wallingford, OX10 8BB, UK

Abstract

Restoring agriculturally degraded habitats to species-rich grasslands is a vital conservation objective. During restoration, how the soil resistome matures alongside microbial community composition and function remains unclear. Here, we tested two competing hypotheses: whether the soil resistome co-occurs through a microbial structural maturation, in which soil restoration is associated with higher-order biotic interactions, or whether antimicrobial resistance (AMR) is instead associated with the competitive pressures and high bacterial taxonomic richness found in disturbed, eutrophic arable land. Using a unique land-use chronosequence on Salisbury Plain, UK, we investigated the trajectory of ecosystem reassembly following the cessation of agricultural activity. Our results demonstrate that AMR abundance increases significantly with restoration age, reaching a maximum in >143-year-old soils. The strongest predictor of this rise in AMR abundance was an increasing microbial eukaryotic signature rather than increasing microbial density, suggesting that resistome expansion is not associated with generalised spatial competition, but rather, co-occurs with structural maturation of the microbiome. We observed an order of magnitude increase in antibiotic biosynthetic potential, dominated by the emergence of streptomycin clusters. Microbial reorientation during soil maturation mirrors the expansion of a core resistome comprised of ancient, intrinsic mechanisms, such as MFS

efflux pumps and RbpA target protection, in older soils. We demonstrate that endogenous AMR is a hallmark of healthy, restored soil ecosystems rather than a marker of anthropogenic soil degradation.

Keywords:

Antimicrobial resistance, soil health, chronosequence, soil restoration, metagenomics, biosynthetic gene clusters, fungal-bacterial ratio

Main

The recovery of plant communities during grassland restoration is comparatively well described[1,2,3], but the maturation of the below-ground microbiome and its resistome during soil recovery remains much less clear. In particular, there is a lack of certainty as to whether the soil resistome reflects disturbance[4], competition[5], and nutrient enrichment[6] in arable systems, or instead emerges as a feature of long-term ecological recovery[7]. This distinction matters because AMR in soils is not solely a product of anthropogenic contamination[8] but is also rooted in ancient microbial interactions[9] and natural secondary metabolism[10]. Following our recent characterisation of chronological soil functional maturation[11] using a multi-generational calcareous grassland restoration chronosequence on Salisbury Plain, UK, we here test how soil resistome composition and abundance change as soils mature from arable land, through restoration, to ancient grassland[12]. Grasslands were classified as arable (0 years; mean organic matter 10% LOI), early regenerating (27 years; 16% LOI), regenerating (63 years; 20% LOI), and ancient (>143 years; 23% LOI) (Supp. Tab. 1). By integrating metagenomic AMR profiles with microbial diversity, microbial biomass markers, eukaryote-to-prokaryote ratio, and biosynthetic gene cluster potential (Supp. Fig. 1, Supp. Methods), we asked whether the soil resistome is associated with disturbed, species-rich arable soils or with the functional maturation of restored ecosystems.

Microbial reorientation, proliferation, and the resistome

Analysis of the metagenomic resistome across the soil chronosequence revealed a progressive accumulation of total AMR gene abundance over time (Fig. 1A, Supp. Fig. 2). Rather than being associated with increasing microbial density, multivariable Generalised Least Squares (GLS) modelling demonstrated that resistome accumulation is strongly predicted by a shift in biotic equilibrium (Fig. 1B). When accounting for soil physico-chemical variations and community covariance, the most robust and significant positive predictor of total AMR gene abundance was the Eukaryote:Bacteria ratio (β = 0.115, P = 0.002), indicating that resistome expansion strongly coordinates with a shift in microbial balance. Other ecosystem features, including soil pH, organic matter, C:N ratio, microbial biomass, and Prokaryotic Simpson's dominance index, remained non-significant within the multivariable framework. The simultaneous increase of AMR and Eukaryote:Bacteria ratio is accompanied by successional transitions across major microbial lineages (Fig. 1C–D). Within the prokaryotic landscape, major phyla exhibit subtle relative shifts, including increases in Verrucomicrobiota alongside changes in key taxa such as Actinomycetota (Fig. 1C). Concurrently, the micro-eukaryotic community experiences a marked expansion in relative abundance of Soil Protists and Basidiomycota (which include key saprotrophic and mycorrhizal fungal guilds) at the expense of specific Ascomycota classes (Fig. 1D). Together, these taxonomic reorientations detail the multi-kingdom structural succession that co-occurs with resistome expansion across the chronosequence.

Successional coupling of antibiotic biosynthetic potential and the resistome

The successional, net increase in the resistome was matched by a tenfold increase in genomic biosynthetic potential. To capture both canonical and novel secondary metabolic pathways, biosynthetic gene clusters (BGCs) were predicted using an integrated pipeline combining antiSMASH v7.0 and GECCO. Predictions were consolidated into a non-redundant union based on overlapping genomic coordinates, ensuring each locus was quantified only once across tools (Supp. Methods). Total BGC abundance increased by an order of magnitude from arable to ancient soils with unique

gene clusters rising from a baseline of ~5 in arable soils to >50 in ancient grasslands (Fig. 2A). This substantial increase in biosynthetic potential is consistent with a plausible ecological basis for the parallel rise in endogenous AMR genes as BGCs and resistance genes are typically co-selected[13] (Fig. 2B; Supp. Fig. 3). Resistome analysis across the chronosequence revealed successional increases in efflux systems (MFS, RND, and ABC transporters) and target protection mechanisms (*RbpA*) which safeguard essential cellular machinery from natural secondary metabolites[14], whilst anthropogenic marker genes, including the class 1 integron integrase gene (*intI1*), sulfonamide resistance genes (*sul1*, *sul2*), disinfectant resistance genes (*qac*), and the human gut/sewage viral marker crAssphage remained below the limit of detection across all restoration sites (Supp. Tab. 2). The enrichment of streptomycin-like BGCs in ancient soils suggests that mature systems harbour a more specialised secondary metabolic potential, a pattern hypothesised to reflect shifting spatial dynamics and ecological interactions between prokaryotic and eukaryotic communities[13].

Conclusion

Our findings challenge the assumption that environmental AMR reflects anthropogenic degradation[8]. Across this 143-year chronosequence reflecting natural regeneration of calcareous grassland, resistome abundance increased alongside broader shifts in microbiome structure and biosynthetic potential, indicating that endogenous AMR can also be a feature of long-term ecological recovery. While primary succession in pristine glacier forelands exhibits early stabilisation of resistance genes driven largely by mobile genetic elements (*intI1*) and horizontal gene transfer[7], our secondary succession model reveals a progressive, multi-century accumulation of intrinsic resistance mechanisms (e.g., MFS efflux, *RbpA*) that tracks with multi-kingdom structural maturation and BGC potential, with mobile element markers remaining below detection. These results highlight the importance of distinguishing natural, restoration-associated resistome signals from those linked to anthropogenic AMR pressure. We observed that clinical markers like rifampin monooxygenase remained static (Supp. Fig. 3), while natural markers linked to soil BGCs were strongly enriched in

mature sites, suggesting that AMR composition and abundance may provide a useful insight into microbiome reassembly and restoration status in calcareous grassland soils. To ensure that our findings, based upon measurements of genetic potential, are representative of active selections and interactions, metatranscriptomics and metabolomics will be required in future studies to definitively capture the phenotypic expression and metabolic kinetics associated with the observed relationships.

Data and code availability

Sequence data is available at NCBI-SRA under BioProject ID: PRJNA1424699. Scripts and data tables are available at https://doi.org/10.5281/zenodo.20396655

Acknowledgments

The authors have no acknowledgments to declare.

Study funding:

UK Research and Innovation:

BBX011089/1 (Earlham Institute's Strategic Programme Grant: Decoding Biodiversity)

NE/S005137/1 (LOCKED UP: The role of biotic and abiotic interactions in the stabilisation and persistence of soil organic carbon)

References

1 Slodowicz, D., Durbecq, A., Ladouceur, E., Eschen, R., Humbert, J.-Y., Arlettaz, R. The relative effectiveness of different grassland restoration methods: A systematic literature search and meta-analysis. *Ecological Solutions and Evidence* 4, e12221 (2023). https://doi.org/https://doi.org/10.1002/2688-8319.12221

2 Poniatowski, D., Stuhldreher, G., Helbing, F., Hamer, U. & Fartmann, T. Restoration of calcareous grasslands: The early successional stage promotes biodiversity. *Ecological*

Engineering 151, 105858 (2020). https://doi.org/https://doi.org/10.1016/j.ecoleng.2020.105858

3 Fagan, K. C., Pywell, R. F., Bullock, J. M. & Marrs, R. H. Do restored calcareous grasslands on former arable fields resemble ancient targets? The effect of time, methods and environment on outcomes. *Journal of Applied Ecology* 45, 1293-1303 (2008). https://doi.org/https://doi.org/10.1111/j.1365-2664.2008.01492.x

4 Zeng, Y., Feng, R., Huang, C., Liu, J. & Yang, F. Antibiotic Resistance Genes in Agricultural Soils: A Comprehensive Review of the Hidden Crisis and Exploring Control Strategies. *Toxics* 13 (2025). https://doi.org/10.3390/toxics13040239

5 Roy, S., Dawson, R. A., Bradley, J. A. & Hernández, M. Prevalence and dynamics of antimicrobial resistance in pioneer and developing Arctic soils. *BMC Microbiology* 25, 50 (2025). https://doi.org/10.1186/s12866-025-03745-7

6 Fu, Y., Hu, F., Wang, F., Xu, M., Jia, Z., Amelung, W., et al. Field-based evidence for the prevalence of soil antibiotic resistomes under long-term antibiotic-free fertilization. *Environment International* 195, 109202 (2025). https://doi.org/https://doi.org/10.1016/j.envint.2024.109202

7 Shen, J.-P., Li, Z.-M., Hu, H.-W., Zeng, J., Zhang, L.-M., Du, S., et al. Distribution and Succession Feature of Antibiotic Resistance Genes Along a Soil Development Chronosequence in Urumqi No.1 Glacier of China. *Frontiers in Microbiology* Volume 10 - 2019 (2019). https://doi.org/10.3389/fmicb.2019.01569

8 Al-Khalaifah, H., Rahman, M. H., Al-Surrayai, T., Al-Dhumair, A. & Al-Hasan, M. A One-Health Perspective of Antimicrobial Resistance (AMR): Human, Animals and Environmental Health. *Life (Basel)* 15 (2025). https://doi.org/10.3390/life15101598

9 D'Costa, V. M., King, C. E., Kalan, L., Morar, M., Sung, W. W. L., Schwarz, C. Et al. Antibiotic resistance is ancient. *Nature* 477, 457-461 (2011). https://doi.org/10.1038/nature10388

10 Perry, E. K., Meirelles, L. A. & Newman, D. K. From the soil to the clinic: the impact of microbial secondary metabolites on antibiotic tolerance and resistance. *Nat Rev Microbiol* 20, 129-142 (2022). https://doi.org/10.1038/s41579-021-00620-w

11 Goodall, T., Busi, S. B., Jones, B., Thorpe, A., Griffiths, R. I., Redhead, J., et al. Taxonomic filtering accompanies functional expansion during long-term soil restoration. *The ISME Journal* (2026). https://doi.org/10.1093/ismejo/wrag131

12 Redhead, J. W., Sheail, J, Bullock, J. M., Ferreruela, A, Walker, K. J., Pywell, R. F. The natural regeneration of calcareous grassland at a landscape scale: 150 years of plant community re-assembly on Salisbury Plain, UK. *Applied Vegetation Science* 17, 408-418 (2014). https://doi.org/https://doi.org/10.1111/avsc.12076

13 Surette, M. D. & Wright, G. D. Lessons from the Environmental Antibiotic Resistome. *Annu Rev Microbiol* 71, 309-329 (2017). https://doi.org/10.1146/annurev-micro-090816-093420

14 Davies, J. & Davies, D. Origins and evolution of antibiotic resistance. *Microbiol Mol Biol Rev* 74, 417-433 (2010). https://doi.org/10.1128/mmbr.00016-10

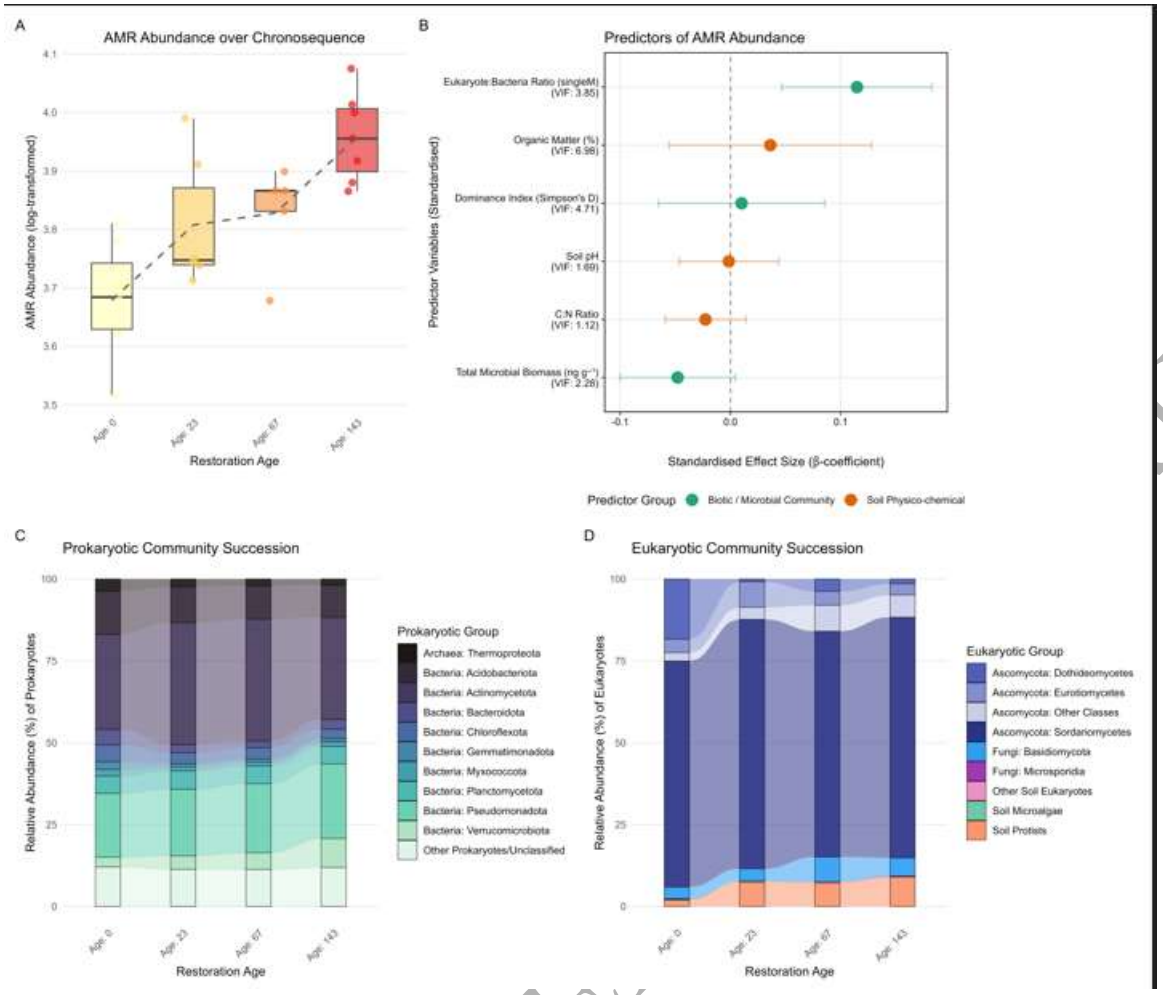

Figure 1. Soil resistome expansion, statistical predictors, and multi-kingdom taxonomic succession across the chronosequence.

(A) AMR Abundance over Chronosequence: Log-transformed total antimicrobial resistance (AMR) gene abundance normalised to Fragments Per Kilobase per Million mapped reads on the Chromosome (log_{10} FPKPMC + 1) and mapped across the soil chronosequence. Box plots indicate the median and interquartile range, individual points represent raw sample replicates (n = 24). The dashed trendline tracks the shift in group means over time.

(B) Drivers of AMR Abundance: Standardized effect size (*β*-coefficient) plot generated from a Generalized Least Squares (GLS) multivariable model evaluating the direct predictors of soil AMR abundance. Horizontal error bars signify 95% confidence intervals. Biotic variables utilize low-variance inflation factor metrics, including Total Microbial Biomass (ng g^{-1} dry soil) derived from microbial-specific phospholipid fatty acid (PLFA) extractions, and the Eukaryote:Bacteria ratio mapped via universal single-copy ribosomal marker genes (singleM) .

(C) Prokaryotic Community Succession (SingleM): Alluvial profile showing the relative abundance transitions (%) of dominant bacterial and archaeal phyla across the restoration timeline.

(D) Eukaryotic Community Succession (Kraken2): Taxonomic succession of the soil eukaryotic community filtered to exclude macro-organism. Fungal reads are partitioned into dominant classes of the Ascomycota phylum (*Sordariomycetes*, *Dothideomycetes*, *Eurotiomycetes*) alongside *Basidiomycota*, *Microsporidia*, and *Soil Protists* to visualize shifting trophic complexity.

Alt-text: Four-panel figure showing soil antibiotic resistance gene (ARG) abundance, statistical predictors, and microbial succession across a soil restoration chronosequence (Ages 0, 23, 67, and 143 years). Panel A shows a box plot of log-transformed AMR gene abundance increasing over time. Panel B shows standardized effect sizes from a GLS multivariable model, where Eukaryote:Bacteria ratio is the only significant positive predictor. Panels C and D show alluvial plots of relative abundance shifts in prokaryotic and micro-eukaryotic taxa across restoration ages.

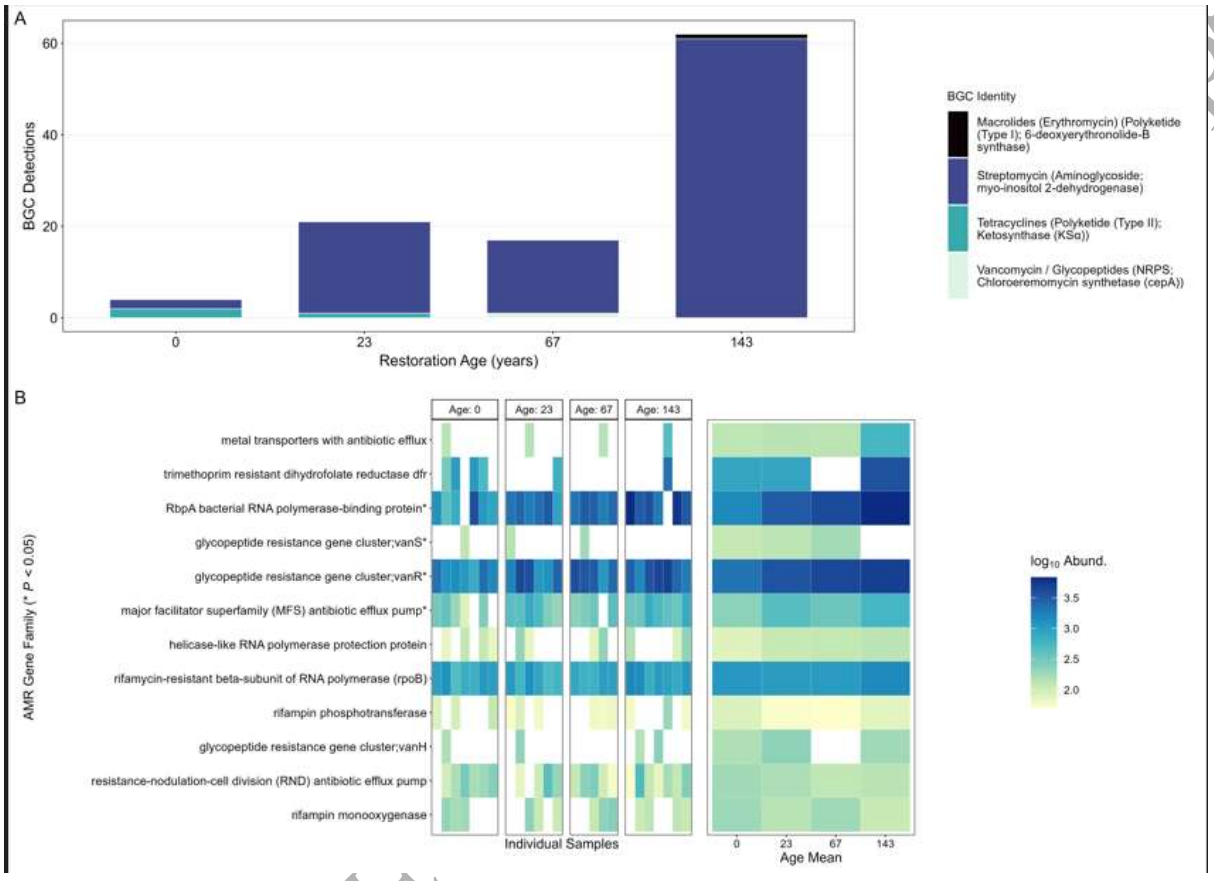

Figure 2. Biosynthetic Gene Clusters (BGCs) and Resistome dynamics across the chronosequence.

(A) Stacked bar plot showing relative abundance and detection profiles of individual Biosynthetic Gene Clusters.

(B) Heatmaps tracking the dynamics of AMR gene families across individual samples (left panel) and their group-level mean log-transformed abundance per restoration age (right panel). Asterisks (*) denote gene families exhibiting statistically significant linear abundance shifts across the chronosequence ($P < 0.05$), and only those with valid linear model slopes are displayed (see Supp. Tab. 2 for full list of detected AMR gene families).

Alt-text: Two-panel figure illustrating biosynthetic gene cluster (BGC) potential and antimicrobial resistance (AMR) gene family dynamics across a soil restoration chronosequence (Ages 0, 23, 67, and 143 years). Panel A shows a stacked bar plot of BGC detections, dominated by a sharp increase in Streptomycin clusters at Age 143. Panel B presents heatmaps tracking log10 abundance of 11 AMR gene families across individual samples and age-group means, highlighting significant linear increases in intrinsic mechanisms such as RbpA, vanS, vanR, and MFS efflux pumps.